UNIVERSITEIT•STELLENBOSCH•UNIVERSITY
jou kennisvennoot • your knowledge partner

Optimisation of a line-start permanent magnet synchronous machine for a load specific application (repository copy)

Article:

Sorgdrager, A.J., Wang, R-J., Pfeffer, A.K., (2015) Optimisation of a line-start permanent magnet synchronous machine for a load specific application, *Proc. of the Southern African Universities Power Engineering Conference*, (SAUPEC), Johannesburg, pp. 216--220, 28-29 January 2015

Reuse
Unless indicated otherwise, full text items are protected by copyright with all rights reserved. Archived content may only be used for academic research.

OPTIMISATION OF A LINE-START PERMANENT MAGNET SYNCHRONOUS MACHINE FOR A LOAD SPECIFIC APPLICATION

A.J. Sorgdrager*, R-J Wang * and A.K Pfeffer

* *Department of Electrical and Electronic Engineering, Stellenbosch University, Private Bag X1, Matieland 7602, South Africa E-mail: ajsorgdrager@gmail.com, rwang@sun.ac.za*

Abstract: This paper presents the design, optimisation and prototyping of a 2.2 kW line-start permanent magnet synchronous motor. The initial design is done using analytical approach based on classical machine theory, which is then optimized. For the optimization, a gradient based Quasi Newton algorithm is used along with generic cost function methodology. The transient performance of the optimal design is evaluated by using transient 2D finite element (FE) time-step modeling. A prototype machine based on the optimal design is manufactured and experimentally evaluated. The simulated and measured results are compared. Relevant discussion and conclusions are drawn.

Key words: Line-start motor; permanent magnet; induction motor; design optimization; finite element method; transient performance; cage winding.

1. INTRODUCTION

Future energy challenges and global environmental concerns urge the world to focus on energy efficiency programs more than ever. Energy efficiency improvement is an important way to address these challenges. Since motor-driven systems are responsible for approximately 70% of all electricity consumption in industry, huge amount of energy saving can be realized by increasing electrical motor efficiency. Although the performance of induction motors have been significantly improved over years, the inherent limitation of induction motors such as relatively poor efficiency and power factor cannot easily be remedied. With the introduction of IEC 60034-30 standard, electrical motor manufacturers worldwide increasingly focuses on alternative motor technologies in an attempt to meet with the forthcoming IE4 standard. Amongst others, line start (LS) permanent magnet synchronous motor (PMSM) technology has received considerable attention. The distinct advantages of LSPM motors such as high efficiency, high power factor and high power density have made this new type of motor very attractive. This paper presents the design, optimisation and prototyping of an interior permanent magnet (PM) radial flux LS PMSM motor for fan-type loads applications.

2. DESIGN PROCEDURE

In this section the procedure of design is discusses. For cost saving purpose, an existing 2.2 kW, 4-pole, 525V, IE3 induction machine stator is used, whose key specifications are listed in Table 1. Essentially, this is a retrofit design with a main focus on the optimal design of the rotor.

2.1 Design Methodology

Fig. 1 illustrates the basic design methodology employed for the design process. The initial design is carried out by using the classical machine theory presented in [1–3].

Table 1: IE3 induction machine stator data.

Description	Specs
Outer diameter, mm	160
Inner diameter, mm	100
Stack length, mm	120
Number of slots	36
Number of turns per slot	81
Connection type	Delta
Air-gap length, mm	0.5
Lamination material	M400-50A

The optimisation criteria is implemented only on the rotor parameters subjecting to some dimension and topology constraints.

Essentially an LS PMSM contains two vastly different machines within one volume. The optimisation of its rotor is a rather complex process involving both cage and PM array design. The cage design mainly influences the transient (asynchronous) operation of the machine whereas the PM array (*PM components, duct and flux barriers*) design is responsible for the steady-state (synchronous) performance. The inherent competition of space between the cage slots and PM arrays often poses significant design challenges in the design of these machines. A simple two-step design approach is often adopted, i.e. (i) an analytical design analysis taking into account asynchronous operation to certain extent is first used to find a suitable design; (ii) after which a 2D FEM time-step analysis is applied to the candidate design to validate its starting and synchronization capability.

One important aspect of this design approach is that the accurate load characterization is necessary. By incorporating the dynamic response of an actual load, the transient performance of the machine can be better inspected and a more accurate comparison can be made once the machine has been experimentally tested against

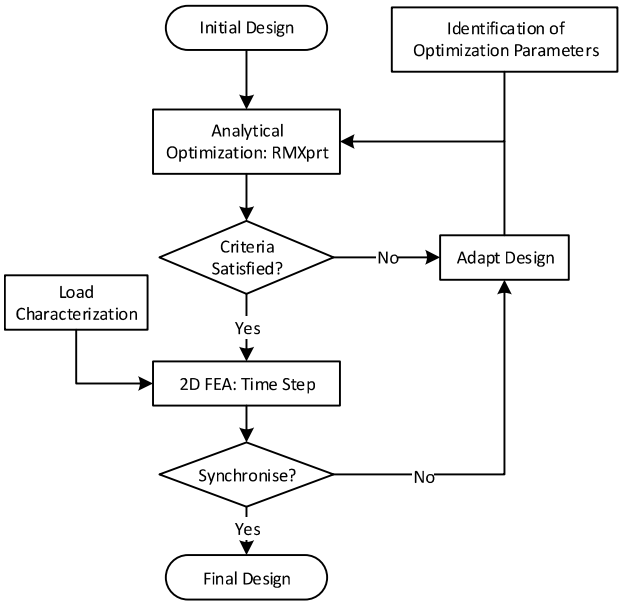

Figure 1: Flowchart of the design procedure

the same load. If the load connected machine synchronizes during the FEM time-step simulation, no further design changes is made and the machine can be manufactured. In the case that the machine fails to synchronize, the design is revisited and a further design iteration is required.

2.2 *Optimisation Algorithm and Criteria*

For the design optimisation, the gradient based Quasi Newton algorithm is employed to search for the minimum value of a defined cost function. The generic format of the cost function is given by (1). The cost value is the sum of the the normalized value around 1 for each performance objective that forms part of the optimisation criteria. The higher the deviation from the target value the higher the cost value. When minimising or maximising an objective, a theoretical limit is used as the target value .Each of the performance objectives is assigned a weight factor , K_i, according to its importance. Table 2 shows the objectives for the optimisation criteria along with their targets and weight values. It is clear that the ideal cost output will be 9.

$$\text{Cost} = \sum_i K_i[1 + |\text{Target Value} - \text{Actual Value}|^2] \quad (1)$$

By including the required rated output power (P_{out}) and rated torque (T_{rated}) in the cost function, it ensures that each machine during the optimisation is a valid design. The synchronous torque of an LS PMSM is calculated in the same manner as a PMSM and is the sum of the magnetic and the reluctance torque. The main torque (*magnetic torque*) is generated by the PM flux interacting with the stator coils. The higher the back-EMF the higher the torque. However, the magnitude of the braking torque developed during the transient operation is also directly proportional to the back-EMF and PM volume [4, 5]. By maximizing the back-EMF and minimizing the PM volume the PM leakage flux is reduced thus utilizing the maximum possible magnetic energy to achieve the desired performance. This prevents the optimizer from increasing PM volume for a higher back-EMF, which also in turn improves the transient performance. The target value for the back-EMF is set in the range as described in [2]. The target limit for the PM mass is calculated by determining the minimum BH operating point energy product to achieve the desired air-gap flux density [1].

Table 2: Composition of the cost function.

Objective	**Goal**	**Weight (K_i)**
T_{rated}	14 Nm	1
P_{out}	2.2 kW	1
back-EMF (rms)	0.9 pu	1
PM mass	Min	2
T_{start}	Max	3
B_{ag}	0.55 T	1

Apart from achieving high efficiency and unity power factor at rated steady state condition with minimal PM volume, the motor needs to develop the highest possible starting torque. This is required to overcome the initial load and braking torque during transient operation. There is however no set criteria for quantifying the starting torque. A general assumption is that the higher the torque, the more likely machine is to synchronize. The starting torque of an LS PMSM is affected by the rotor slot profiles such as slot shape, depth, width and area.

The specific weight assigned to each objective is according to the importance each objective has on the overall optimisation criteria. By adding more weight to the PM volume and starting torque in the cost function, the optimisation is conducted with more consideration on the transient performance.

2.3 *Optimisation Variables*

As stated before, an LS PMSM has a hybrid rotor. In the rotor cage design, the total number of slots are selected as 28, which is the same as that of an IM with the same power rating. However a round slot is used as shown in Fig. 2 for the following reasons: (i) firstly, from a manufacturing point of view, if the rotor bars casting is not available, the round rotor bars can be easily manufactured and inserted into the slots; (ii) secondly, the number of variables to characterize a round slot in the optimisation is reduced to merely three.

Fig. 3 illustrates the different parameters that define the PM slot. The PM width (W_m) can vary within the width of the slot but its thickness (T_m) should match that of the slot. The gap between two PM slots (Rib) and the nearby cage slot bottom region form a flux saturation zone to limit the PM leakage flux. By optimally designing saturation zones, the magnet utilization factor can be much improved. By varying the depth of the PM slot (O1) along with the PM width, a suitable air-gap flux density can be realized [7].

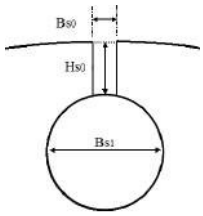

Figure 2: Rotor slot dimensions

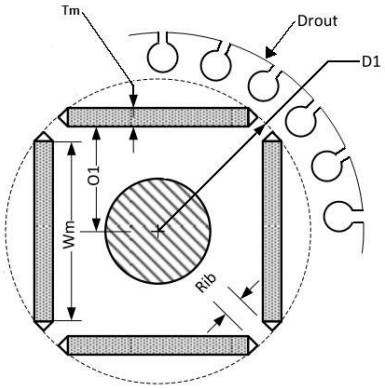

Figure 3: Magnet and PM slot dimensions

2.4 *Optimized Design*

Table 3 contains the relevant information of each variable. The starting values are the initial machine design that was calculated analytically as in [1]. The total number of simulations for the optimization is 408. Table 4 summarizes the change of each objective between the initial and optimized machines and Figs. 4 to 6 compare the different torque components. It is clear that optimized machine outperforms the initial design. The better utilization of the PM material increases both the air-gap flux density and back-EMF resulting in a higher maximum torque at steady-state as shown in Fig. 4. The higher back-EMF causes a higher braking torque, which is expected.

As the optimisation criteria is satisfied, the next step is to inspect the synchronization capability of the optimized machine with a specific load. For this project, a custom designed axial fan is used as the specific load, which provides a load torque of 14 Nm at the rated speed of 1500 rpm. The fan's torque-speed curve, moment of inertia and damping coefficient are experimentally determined and implemented in ANSYS' Maxwell 2D FEM software. Fig. 7 is a flux density plot of the final design under full load condition at a certain time-step. Fig. 8 shows the

Table 3: Optimisation topology parameters.

Variable	Start Value	Min	Max
Bs0	1.5	1	3
Bs1	6.4	6	7
Hs0	3	1.325	3
D1	77	63	78
O1	24	23	27
Rib	2.5	2	4
T_m	6.5	4	7
W_m	30	28	35

Table 4: Cost function objective comparison

Objective	Goal	Initial	Optimised
T_{rated}, Nm	14	14	14
P_{out}, kW	2.2	2.2	2.2
EMF (rms), V	370	330	341
PM mass, kg	Min	0.755	0.581
T_{start}, Nm	Max	47.89	54.56
B_{ag}, T	0.55	0.50	0.53

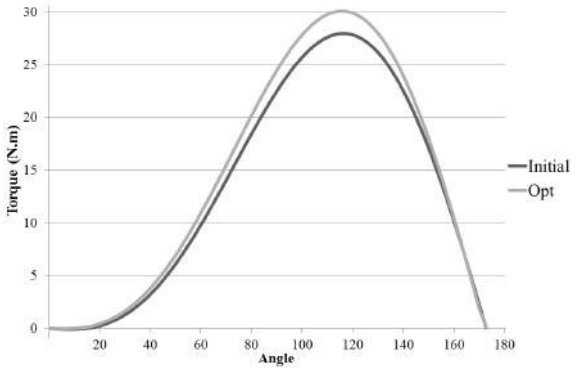

Figure 4: Comparison of initial and optimum steady-state torque

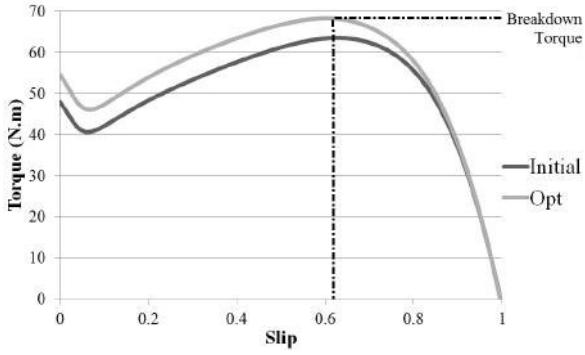

Figure 5: Comparison of initial and optimum torque-slip characteristics

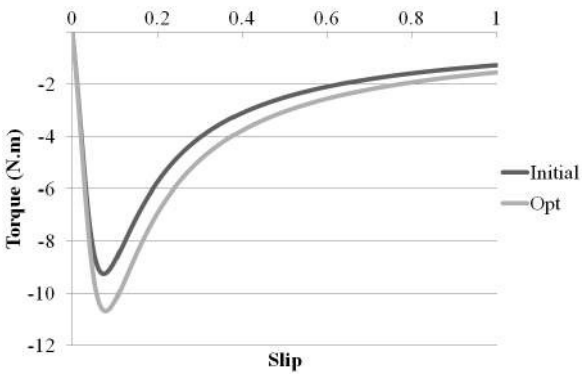

Figure 6: Comparison of initial and optimum braking torque

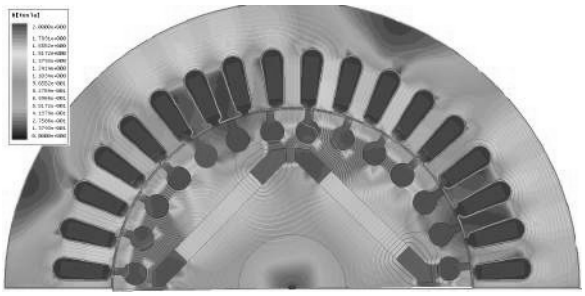

Figure 7: Steady-state flux density plot

transient synchronization performance of the optimized machine. From the figure it is clear that rated speed is reached at $\pm$ 0.8 s and the decision was made to manufacture the rotor.

3. SIMULATION AND EXPERIMENTAL RESULTS

This section compares the measured and simulated results of the machine in terms of the no-load, full-load and transit performance. Table 5 compares the simulated and the actual performance for both no-load and load test. The simulated performance shows high efficiency operating at a good power factor. The full load line current is also lower than an IE3 induction machine of the same rating.

It was possible during manufacturing to cast the rotor bars and end rings using gravity casting. The preferred method of casting, as used by electrical machine manufacturers, is vacuum pressure injection, but this is very costly for prototype manufacturing. To use gravity casting, the stack and casting jig have to be preheated before pouring in the aluminum. This is to prevent the aluminum from setting too quickly and creating air voids in aluminum bars. Once the aluminum cooled the stack can be removed from the casting jig and machined to provide the required air-gap. An image of the prototype rotor is shown in the Appendix

3.1 Performance Evaluation

To inspect the synchronization capabilities of the machine, the start-up test of the machine with the fan load is conducted in the laboratory. The machine failed to reach synchronization and settled at a sub-synchronous speed of 1290 rpm as seen in Fig. 8. The figure provides a comparison between the simulated and measured start-up performances. The measured results correlate well with the simulated ones up to 900 rpm where the two

Table 5: Comparison of measured and simulated results

Description	**Simulated**	**Measured**
Efficiency	94.6	-
Power Factor	0.91	-
I_{noload}, A	2.2	2.96
$I_{full\ load}$, A	3.93	9.56
$T_{average}$, Nm	14	14.5
Speed, rpm	1500	1290

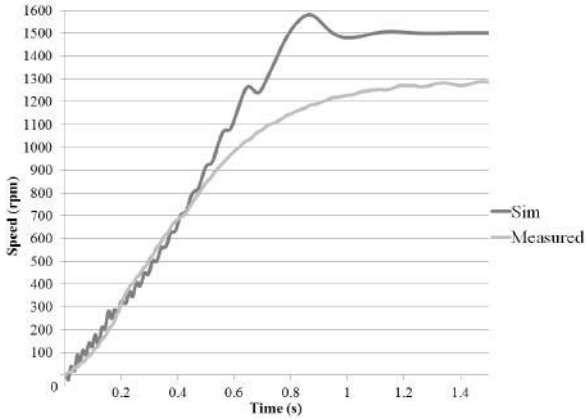

Figure 8: Comparison of measured and predicted start-up speed versus time characteristics of the LS PMSM

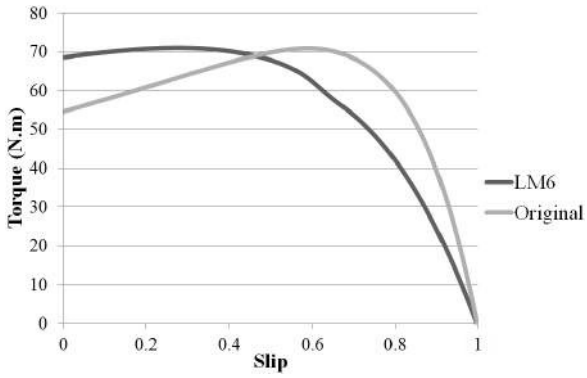

Figure 9: Torque curve deviation due to aluminium grades used

curves start to diverge. Upon further investigation it was determined that the main cause of the failed synchronisation is due to the aluminium grade used to cast the rotor cage, namely LM6. This aluminium grade has a lower electrical conductivity than the one selected during the design phase thus resulting in a higher resistance. This resulted in a change in transient torque as seen in Fig 13. A slight torque dip can also bee seen between 0.6 to 0.7 which is around the diverge speed point. The increase resistance moved the breakdown torque point further away from $s = 1$ and as a result the PM cannot generate enough pull-in torque to bring the rotor into synchronization. As a result, the rotor operates at a sub-synchronous speeds. Under such an operation condition, the machine develops a pulsating torque and line current as shown in Figs 10-11.

Since the prototype machine failed to synchronize, the efficiency and power factor of the machine could not be determined for rated performance. The full load measurements could not be completed as the excessive line currents trip the protection breakers before the Watt-meters can be switched in. These Watt-meters cannot handle the high inrush staring currents so that they can only be switched in after the start up. In addition to the performance tests, the back-EMF waveform of the machine is also measured and compared to the simulation one. The measured and simulated waveform magnitude show significant discrepancy as seen in Fig. 12.

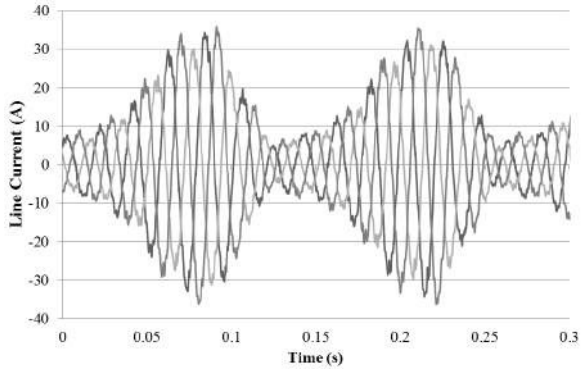

Figure 10: Instantaneous current waveform of LS PMSM under sub-synchronous speed

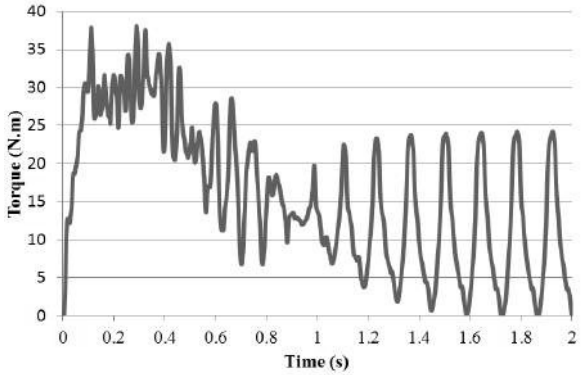

Figure 11: Instantaneous torque waveform of the LS PMSM under sub-synchronous speed

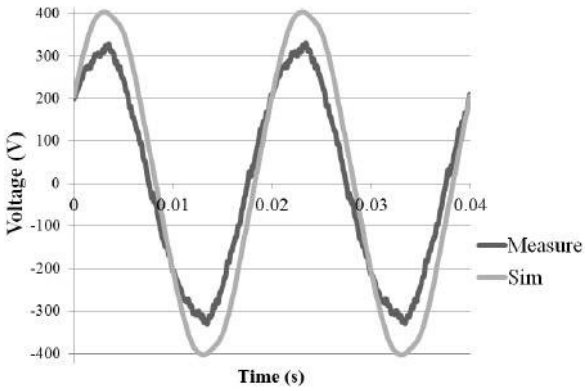

Figure 12: Measured and predicted back-EMF voltage of the LS PMSM prototype

4. CONCLUSION

The paper presents a design optimisation approach for an LS PSMS using a gradient based cost function to maximize starting torque and minimize PM volume whilst still adhering to a high steady state performance. The synchronization capability of the machine is checked using a 2D FEA time step simulation that incorporates the load parameters of the fan load set-up. The simulation results show good steady state and transient performance. The manufactured prototype machine was unable to synchronize when driving the load and as a result the simulated and actual machine performance differed. Further investigation is still required into incorporating load parameters in a time step simulations before a conclusion can be made on the optimisation approach.

REFERENCES

[1] A.J. Sorgdrager, A.J. Grobler, and R-J Wang, Design Procedure of a Line-Start Permanent magnet synchronous machine, in Proc. of the 22nd South African Universities Power Engineering Conference, 2014, vol. 22, no. 1, pp. 307-314.

[2] J. Pyrhonen, T. Jokinen and V. Hrabovcová, Design of rotating electrical machines, (1st ed.) West Sussex, United Kingdom: John Wiley & Sons, Ltd, 2008.

[3] I. Boldea and L. Tutelea, Electric machines, (1st ed.) USA:CRC Press, 2010.

[4] V.B Honsinger, "Permanent Magnet Machines: Asychronous Operation", IEEE Trans. on Power Apparatus and Systems, vol. PAS-99, vol. 4, pp. 1503-1509, 1980

[5] F.J.H. Kalluf, C. Pompermaier, M.V.F. Da Luz, and N. Sadowski, Braking torque analysis of the single phase line-start permanent magnet synchronous motor, in International Conference on Electrical Machines (ICEM), 2010, pp. 2011-2011.

[6] A. Isfahani and S. Vaez-Zadeh, Effects of magnetizing inductance on start-up and synchronization of line-start permanent-magnet synchronous motors, IEEE Trans. on Magnetics, vol. 47, no. 4, pp. 823-829, 2011.

[7] A.J. Sorgdrager and A.J. Grobler, Influence of magnet size and rotor topology on the air-gap flux density of a radial flux PMSM, 2013 IEEE Int. Conf. Ind. Technol., pp. 337-343, Feb. 2013.

APPENDIX

Figure 13: Prototype LS PMSM rotor